Segmentation of Retinal Ganglion Cells From Fluorescent Microscopy Imaging

Silvia Baglietto[1,2], Ibolya E. Kepiro[3], Gerrit Hilgen[4], Evelyne Sernagor[4], Vittorio Murino[1,5] and Diego Sona[1,6]

[1]*Pattern Analysis and Computer Vision, Istituto Italiano di Tecnologia, Genova, Italy*

[2]*Department of Naval, Electric, Electronic and Telecommunication Engineering, University of Genova, Genova, Italy*

[3]*Nanophysics, Istituto Italiano di Tecnologia, Genova, Italy*

[4]*Institute of Neuroscience, Newcastle, Newcastle-upon-Tyne, U.K.*

[5]*Department of Computer Science, University of Verona, Verona, Italy*

[6]*NeuroInformatics Laboratory, Fondazione Bruno Kessler, Trento, Italy*

Keywords: Cell Segmentation, Active Contour, Multiscale Blob Filtering, Retinal Ganglion Cell.

Abstract: The visual information processing starts in the retina. The working mechanisms of its complex stratified circuits, in which ganglion cells play a central role, is still largely unknown. Understanding the visual coding is a challenging and active research area also requiring automated analysis of retinal images. It demands appropriate algorithms and methods for studying a network population of strictly entangled cells. Within this framework, we propose a combined technique for segmenting retinal ganglion cell (RGC) bodies, the output elements of the retina. The method incorporates a blob enhancement filtering in order to select the specific cell shapes, an active contour process for precise border segmentation and a watershed transform step which separates single cell contours in possible grouped segmentations. The proposed approach has been validated on fluorescent microscopy images of mouse retinas with promising results.

1 INTRODUCTION

The retina is a photosensitive membranous tissue lying at the back of the eye. Its role is to process the light stimuli and to transmit the information to the brain through the optic nerve. Although it is often compared to a photographic film on which the images are imprinted and encoded into electrical signals with a columnar processing, the retina has a very complex function and structure, composed of several layers of cells in a tangled network (Gregory, 2015): photoreceptors feed into bipolar and amacrine cells, which pass the input to an assorted set of retinal ganglion cells (RGCs). Recent studies show that retina performs sophisticated non-linear computation, extracting spatio-temporal visual features with high selectivity. This is reflected by the fact that distinct RGC types have been found to encode specific visual features for transmission to the brain (Neumann et al., 2016).

According to the current knowledge, there is a correlation between RGC morphology and function and this is usually studied at the single cell level (Berson et al., 2010). Recently, an intense debate is rising around the importance of studying the retina at the circuit level and the actual challenge is to tackle the problem at a different scale, analyzing populations of neurons at a network level (Roska et al., 2006), (Kim et al., 2010). Several studies are trying to model responses of RGC populations heading to a better understanding of the role of RGCs (Baden et al., 2016). To support neuroscientists in this study, automated tools for the large-scale segmentation of RGC bodies are required.

In this work we propose an automatic algorithm for cell segmentation from fluorescent images recorded with a confocal microscope. This process would allow the characterization of different RGC types distinguished by different soma morphologies at the population level, inspiring studies addressing the correlation between soma morphology and functional behavior.

Such datasets are complex for many reasons. They are affected by low contrast at the cell boundaries,

Baglietto S., Kepiro I., Hilgen G., Sernagor E., Murino V. and Sona D.
Segmentation of Retinal Ganglion Cells From Fluorescent Microscopy Imaging.
DOI: 10.5220/0006110300170023
In *Proceedings of the 10th International Joint Conference on Biomedical Engineering Systems and Technologies (BIOSTEC 2017)*, pages 17-23
ISBN: 978-989-758-215-8

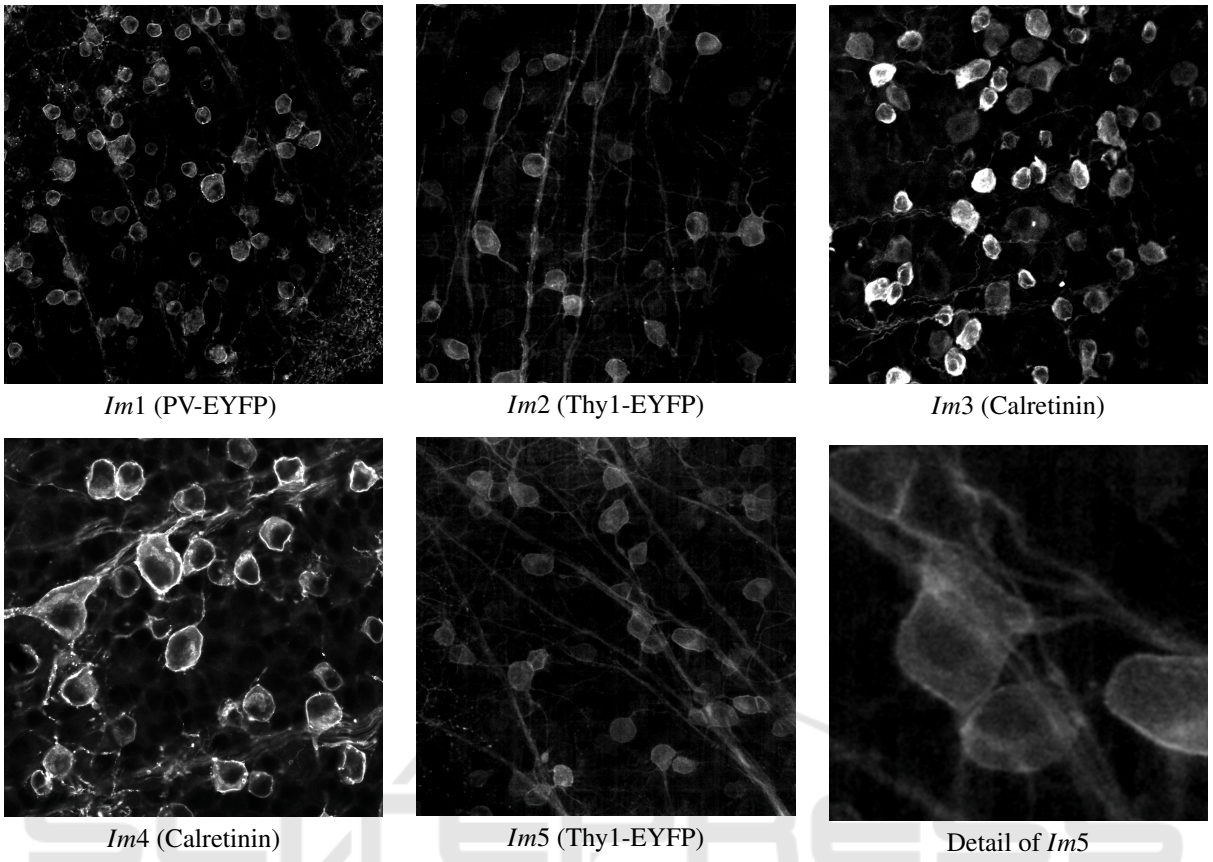

Figure 1: 5 different images containing RGCs used for testing the proposed method. The images show high variability across samples. In the bottom right, there is a magnified crop of *Im*5, showing the complexity of images, where the analyzed structures are mixed with background and other structures.

high cell density and shape deformations, occlusions among neurons and the presence of a large mass of other structures such as dendrites and axons on the same channel. Indeed, the fluorescence in retinal mice images, as shown in Fig.1, is expressed by the whole cell including processes (i.e. dendrites and axons) and it is non-uniform leading to fragmented appearance of the objects and to unreliable separation between somas, dendrites and axons. Last but not least, there is a high variability of samples condition across different acquisitions.

This global setting introduces to new challenging computational tasks for image segmentation. Indeed, state-of-the-art methods usually work on single neuron reconstruction (Gulyanon et al., 2016) and can hardly be adequate for separating neurons from the background. The automated segmentation is still a critical open problem. On the other hand, the manual interaction to generate the morphological reconstruction is time consuming and expensive. Traditional segmentation approaches which use only basic techniques, such as morphological operators and thresholding, are not powerful enough and lead to wrong segmentations (Meijering, 2012). Learning approaches, such as (Arteta et al., 2013) and (Zhang et al., 2014), require hand-labelled neurons for training and testing. In addition, they cannot manage to extract the precise segmentation of cells because of the difficulties dealing with the high variance in cell appearance. In contrast, active contour methods have demonstrated good performance in image segmentation dealing with challenging data (Chan et al., 2001), (Yezzi et al., 2002). Their main limitation is related to the strong sensitivity to the model initialization, which usually requires variable degrees of user intervention. To this end, recent years have witnessed the spread of active contour models in different formulations, aiming at hybrid approaches for automating the initialization process (Ge et al., 2015), (Wu et al., 2015).

Within this scenario, we designed a method based on active contour initialized on specific ROIs, which are automatically identified by a multiscale blob filter emphasizing only cell bodies. Several shape-based

enhancement filters have been introduced in literature. Frangi filter has been reported to be one of the most effective vessel enhancement filter (Frangi et al., 1998). In light of that, we introduced a novel multiscale blob filtering method derived from the Frangi filter for the enhancement of neuron somata. Cell bodies are then segmented by a localizing region-based active contour algorithm (Lankton and Tannenbaum, 2008) followed by a watershed-based step to split groups of neurons and to separate cells from dendrites and axons.

The remainder of the paper is organized as follows. In Sec.2 details on the adopted retinal images are provided. We present the pipeline of our method in Sec.3. In Sec.4 results are discussed and conclusions are provided in Sec.5.

2 MATERIALS

Mouse retinal samples were imaged using Leica SP5 upright confocal microscope. Images were acquired at (sub)cellular resolution and at high averaging number to reduce the noise level due to limited light penetration in deep layers of the tissue where RGCs are located. A total of 5 images (2048×2048 and 1024×1024 pixels), containing some hundreds of cells, were selected from 3 different retina samples including: i) three images coming from samples with genetic fluorescence expression, (i.e., $Im1$ from PV-EYFP and $Im2$ and $Im5$ images from Thy1-EYFP mouse), and ii) two images from samples with immunofluorescence staining using the Calretinin calcium-binding protein ($Im3$ and $Im4$) (Fig.1-2). The samples were selected in order to best capture the variability in terms of fluorescence expression, cell and axonal bundle density and background.

3 METHOD

There are mainly three steps in our pipeline as shown in Fig.2: Multiscale Blob enhancement filtering (Fig 2.b), Localizing Region-Based Active Contour (Fig 2.c) and Watershed Transform (Fig 2.d).

The blob enhancement filtering is used to initialize the high performance active contour method, heavily dependent on the initialization mask. Thanks to this filter, the processing pipeline can proceed without user intervention and manual adjustment. After blob filtering, the detected blob-shaped objects are binarized and used as initialization ROIs for a localizing region-based active-contour that segments cell borders. In the most challenging images, the active contour can result in cell clusters due to fuzzy cell boundaries and occlusions. In order to overcome this issue, we use the watershed transform.

3.1 Multiscale Blob Enhancement Filtering

The aim of blob enhancement is to improve the intensity profile of RGC bodies and reduce the contribution of dendritic and axonal structures. It is based on the multiscale analysis of the eigenvalues of the Hessian matrix to determine the local likelihood that a pixel belongs to a cell, i.e. to a blob structure. The proposed approach is inspired by the work of Frangi et al. (Frangi et al., 1998) on multiscale vessel enhancement filtering. The Frangi filter essentially depends on the orientational difference or anisotropic distribution of the second-order derivatives to delineate tubular and filament-like structures. We start from this idea and modify the filtering process (in particular equation (15) in (Frangi et al., 1998)) in order to have a reduction of line-like patterns in favor of blob-like structures (as (Liu et al., 2010)). Instead of a vesselness measure, we define a blobness measure as follows:

$$B(x_o) = \begin{cases} 0, & \text{if } \lambda_1^{x_o} < 0 \\ e^{\frac{1}{2\beta^2} \cdot \left(\frac{\lambda_2^{x_o}}{\lambda_1^{x_o}}\right)^2}, & \text{otherwise} \end{cases} \quad (1)$$

where $\lambda_1^{x_o}$ and $\lambda_2^{x_o}$ are the eigenvalues of the Hessian matrix at point x_o and β is a threshold which controls the sensitivity of the blob filter. Both β and the Hessian scale have been selected in the range of the average neuron radius. Eq.(1) is given for bright structures over dark background. In case of dark objects conditions should be reversed.

3.2 Localizing Region-based Active Contour

Localizing region-based active contour (Lankton and Tannenbaum, 2008) is an improved version of traditional active contour models (Chan et al., 2001), (Yezzi et al., 2002) where objects characterized by heterogeneous statistics can be successfully segmented thanks to localized energies, differently from the corresponding global ones which would fail. This framework allows to remove the assumption that foreground and background regions are distinguishable based on their global statistics. Indeed the working hypothesis is that interior and exterior regions of objects are locally different. Within this framework, the energies

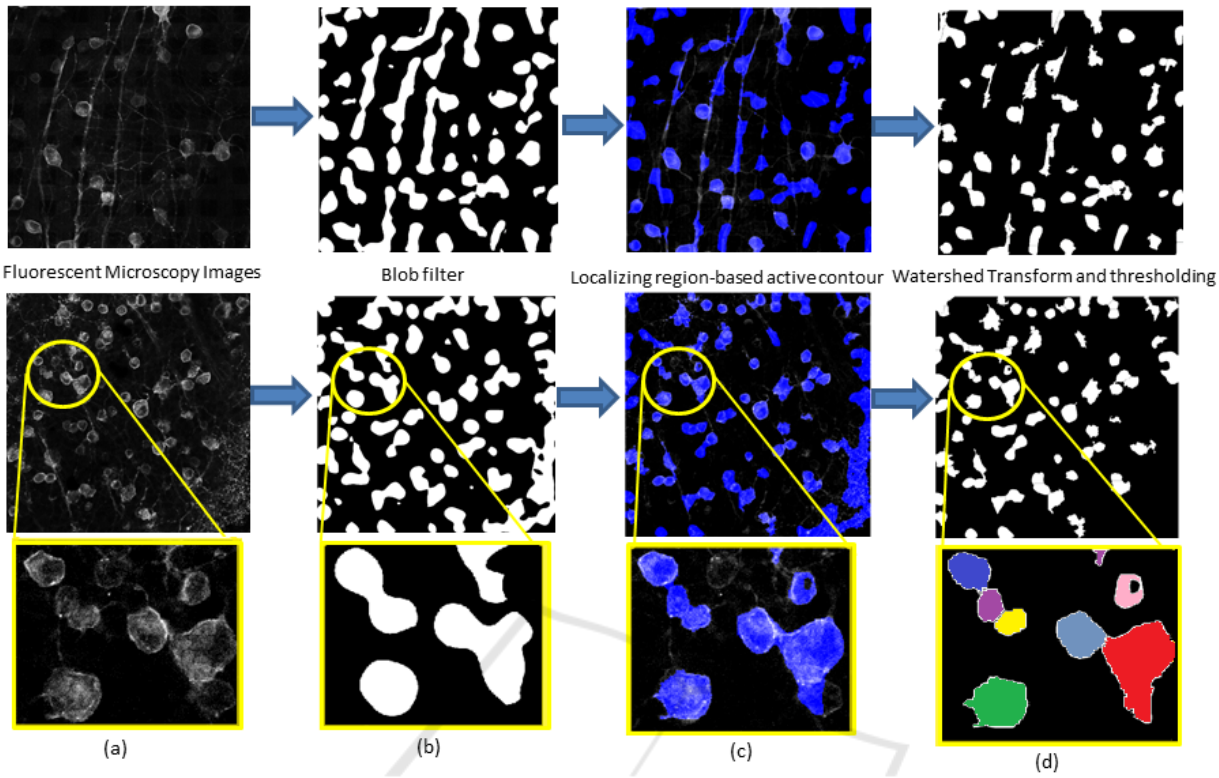

Figure 2: Pipeline applied to two examples (from the top, *Im*2 (Thy1-EYFP) and *Im*1 (PV-EYFP)) with a crop in the bottom line, showing a problem due to contiguous cells. In column, (a): Original Fluorescent Microscopy Images; (b) Results of the blob filter binarization; (c) Results of the active contour segmentation in blue transparency over the original image for getting the suitable qualitative performance; (d) Results of the watershed transform and of the final threshold.

are constructed locally at each point along the curve in order to allow the analysis of local regions. The choice of the localization radius is driven by the size of the object to be segmented. In our case, for each image, we used a radius equal to the average soma radius, which depends on the image size and on the microscope lens.

Thanks to this efficient technique, we obtain a segmentation mask which tightly fits real cell bodies.

3.3 Watershed Transform and Size Filter

The above active contour fails to separate groups of overlapping or contiguous cells, hence we exploit the simplicity and computational speed of the watershed transform, introduced by Beucher and Lantuéjoul (Beucher and Lantuéjoul, 1979).

As a final step, we need to delete components which are too small or too large for being cell somata (a given example is in Fig.2.c (middle figure) by applying a size filter to remove structures with size outside an acceptable range of somata dimensions.

4 RESULTS AND DISCUSSION

We applied our pipeline to 5 different retinal images representative of possible variations on the retinal samples, such as brightness, intensity, size and number of cells, presence of axonal structures and processes, strong background signals, etc. We generated the ground truth manually segmenting all cells in each image (around 280 cells). To give a qualitative evaluation, we report different examples in Fig.2-3 where it is possible to see that our approach works in different sample conditions. To quantify the performance of our method, we adopt the Dice Coefficient (DC), a widely used metric for comparing the ground truth to the computer-aided segmentation. DC is defined as follows:

$$DC = \frac{2(A \cap B)}{(A + B)},$$

where A is the binary ground truth mask and B is the binary segmentation result. The DC value ran-

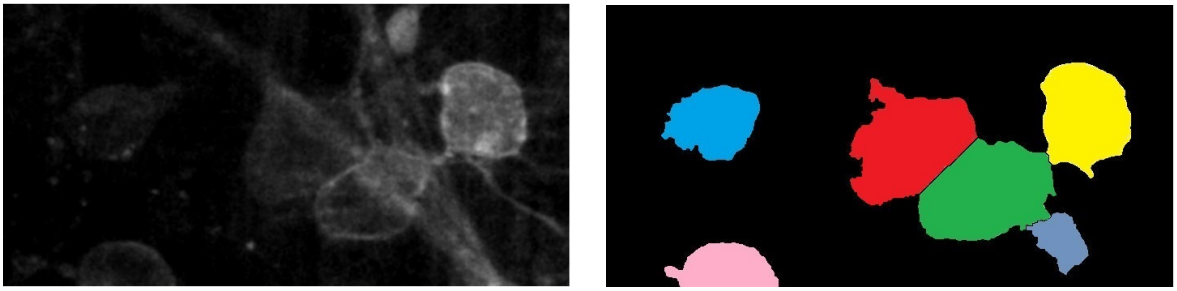

Crop of *Im*5 Resulted Crop Segmentation

Figure 3: Some cells are not easily visible to the human eye just visualizing the retina images, but they are discovered and segmented by our algorithm (for example, in this cropped figure, pink and blue cells were hardly detectable). Adding contrast to the image makes these somata clearer but it increases noise and cell heterogeneity.

Table 1: Segmentation process results. Dice Coefficient has been computed after all steps in the pipeline (Blob Filter, Active Contour and Watershed Transform) and shows improvements after each step. For the final stage of the pipeline, there is also the percentage of detected cells computed assuming as detected a cell with minimum overlap with ground truth fixed at 50%.

Image	# of cells	Blob Filter	Active Contour	Final	
		DC	DC	DC	detected cells
*Im*1 (PV-EYFP)	95	0.60	0.69	0.81	86.32%
*Im*2 (Thy1-EYFP)	37	0.43	0.58	0.64	89.19%
*Im*3 (Calretinin)	64	0.62	0.82	0.83	75.00%
*Im*4 (Calretinin)	29	0.57	0.71	0.79	82.76%
*Im*5 (Thy1-EYFP)	48	0.51	0.62	0.70	85.42%

ges between 0 (absence of agreement) and 1 (perfect agreement). A DC higher than 0.70 usually indicates a satisfactory segmentation (Zijdenbos et al., 1994).

As an additional index of performance, we also provide the percentage of detected cells for each image. We consider a cell as detected if it is correctly segmented for more than 50% of its total area, comparing the segmentation mask to the ground truth for each annotated RGC. Fig.4 shows that 50% threshold is a good trade off between the certainty of a cell detection and a satisfactory retrieval.

Table 1 shows the quantitative results of these metrics on our samples. We compute the DC for each of the three steps. Each stage clearly improves the segmentation, reaching satisfactory results for all images. In *Im*3 (Fig.1), the fluorescence is mainly expressed by the body cells; for this reason, we reach good scores right after the first two steps. The weaker DC values on images *Im*2 and *Im*5 are due to a strong presence of axonal structures which can be hardly removed.

5 CONCLUSIONS

In this paper we have proposed a new algorithm for the large-scale segmentation of cells in challenging retinal images. First, a novel and effective multiscale blob filter is employed for cell enhancement which selects ROIs for the initialization of an active contour step, addressing the known weakness of these methods. Active contour reaches suitable results but needs a further segmentation in case of multiple cell aggregations, which has been addressed using a watershed transform followed by a filter guided by the size of structures.

We validated our approach against manual segmentations on 5 images in which there are some hundreds of neurons representative of a variety of cell appearances and image conditions.

Thanks to its generality, this approach could be applied to similar cell segmentation scenarios and opens new perspectives for the analysis and the characterization of the retinal morphology at a population level.

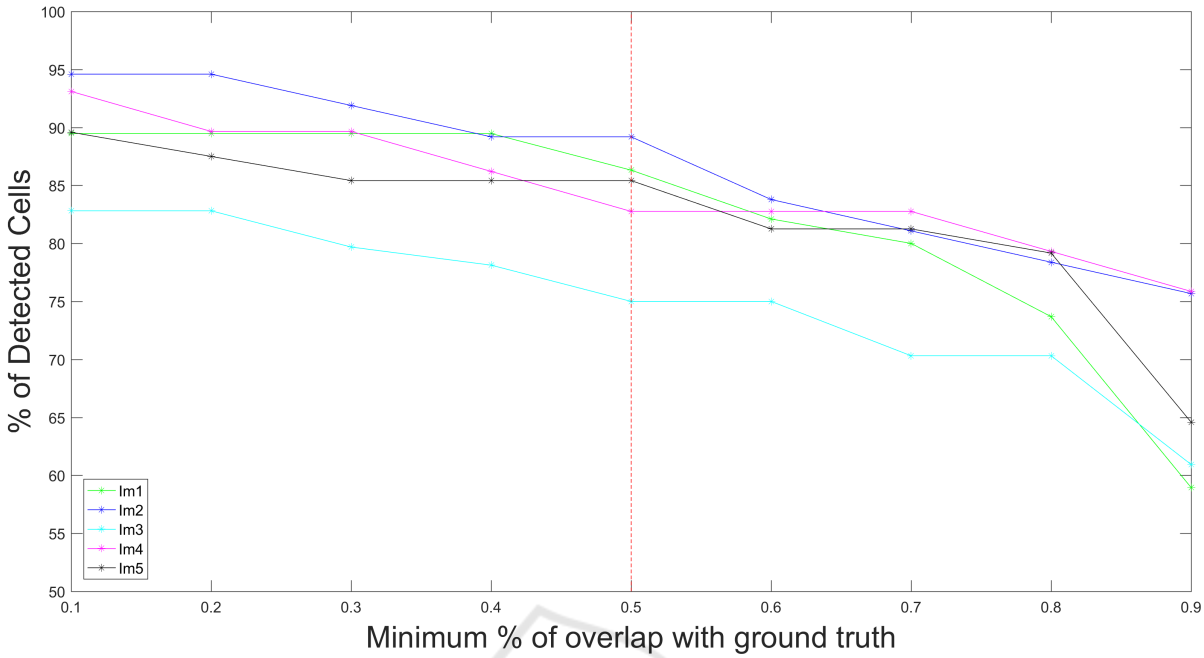

Figure 4: Variation of the % of detected cells as a function of the % of overlap between detected cell and the corresponding annotated ground truth.

ACKNOWLEDGEMENTS

The research received financial support from the 7th Framework Programme for Research of the European Commision, Grant agreement no. 600847: RENVISION project of the Future and Emerging Technologies (FET) programme.
We would like to thank Dr. Luca Berdondini, Dr. Alessandro Maccione, and Dr. Stefano Di Marco (Neuroscience and Brain Technologies, Istituto Italiano di Tecnologia, Genova) for providing the CMOS devices and for their support in the sample preparation. We would also like to thank Dr. Francesca Cella Zanacchi (Nanophysics, Istituto Italiano di Tecnologia, Genova) for her support in the microscopy acquisitions.

REFERENCES

Arteta, C., Lempitsky, V., Noble, J. A., and Zisserman, A. (2013). Learning to detect partially overlapping instances. In *Computer Vision and Pattern Recognition (CVPR), 2013 IEEE Conference on*.

Baden, T., Berens, P., Franke, K., Rosón, M. R., Bethge, M., and Euler, T. (2016). The functional diversity of retinal ganglion cells in the mouse. *Nature*, 529(7586):345–350.

Berson, D. M., Castrucci, A. M., and Provencio, I. (2010). Morphology and mosaics of melanopsin-expressing retinal ganglion cell types in mice. *Journal of Comparative Neurology*, 518(13):2405–2422.

Beucher, S. and Lantuéjoul, C. (1979). Use of watersheds in contour detection. In *International workshop on image processing, real-time edge and motion detection*.

Chan, T. F., Vese, L., et al. (2001). Active contours without edges. *Image processing, IEEE transactions on*, 10.

Frangi, A. F., Niessen, W. J., Vincken, K. L., and Viergever, M. A. (1998). Multiscale vessel enhancement filtering. In *Medical Image Computing and Computer-Assisted InterventationMICCAI98*, pages 130–137. Springer.

Ge, Q., Li, C., Shao, W., and Li, H. (2015). A hybrid active contour model with structured feature for image segmentation. *Signal Processing*, 108:147–158.

Gregory, R. L. (2015). *Eye and Brain: The Psychology of Seeing: The Psychology of Seeing*. Princeton university press.

Gulyanon, S., Sharifai, N., Kim, M. D., Chiba, A., and Tsechpenakis, G. (2016). Crf formulation of active contour population for efficient three-dimensional neurite tracing. In *2016 IEEE 13th International Symposium on Biomedical Imaging (ISBI)*, pages 593–597. IEEE.

Kim, I.-J., Zhang, Y., Meister, M., and Sanes, J. R. (2010). Laminar restriction of retinal ganglion cell dendrites and axons: subtype-specific developmental patterns revealed with transgenic markers. *The Journal of Neuroscience*, 30(4):1452–1462.

Lankton, S. and Tannenbaum, A. (2008). Localizing region-

based active contours. *Image Processing, IEEE Transactions on*, 17(11):2029–2039.

Liu, J., White, J. M., and Summers, R. M. (2010). Automated detection of blob structures by hessian analysis and object scale. In *Image Processing (ICIP), 2010 17th IEEE International Conference on*, pages 841–844. IEEE.

Meijering, E. (2012). Cell segmentation: 50 years down the road [life sciences]. *Signal Processing Magazine, IEEE*, 29(5):140–145.

Neumann, S., Hser, L., Ondreka, K., Auler, N., and Haverkamp, S. (2016). Cell type-specific bipolar cell input to ganglion cells in the mouse retina. *Neuroscience*, 316:420 – 432.

Roska, B., Molnar, A., and Werblin, F. S. (2006). Parallel processing in retinal ganglion cells: how integration of space-time patterns of excitation and inhibition form the spiking output. *Journal of Neurophysiology*, 95(6):3810–3822.

Wu, P., Yi, J., Zhao, G., Huang, Z.and Qiu, B., and Gao, D. (2015). Active contour-based cell segmentation during freezing and its application in cryopreservation. *Biomedical Engineering, IEEE Transactions on*, 62(1):284–295.

Yezzi, A., Tsai, A., and Willsky, A. (2002). A fully global approach to image segmentation via coupled curve evolution equations. *Journal of Visual Communication and Image Representation*, 13(1):195–216.

Zhang, C., Yarkony, J., and Hamprecht, F. A. (2014). Cell detection and segmentation using correlation clustering. In *Medical Image Computing and Computer-Assisted Intervention–MICCAI 2014*, pages 9–16. Springer.

Zijdenbos, A. P., Dawant, B. M., Margolin, R., Palmer, A. C., et al. (1994). Morphometric analysis of white matter lesions in mr images: method and validation. *Medical Imaging, IEEE Transactions on*, 13(4):716–724.